Fenton-like reaction enhanced the CO_2 capture performance of biomass carbon

Xiaoran He
Water and Environmental Engineering Laboratory, Interdisciplinary Graduate School of Engineering Sciences, Kyushu University

Taibao Zhao
International Institute for Carbon-Neutral Energy Research (WPI-I2CNER), Kyushu University

Md. Amirul Islam
International Institute for Carbon-Neutral Energy Research (WPI-I2CNER), Kyushu University

Bidyut Baran Saha
International Institute for Carbon-Neutral Energy Research (WPI-I2CNER), Kyushu University

他

出版情報：Proceedings of International Exchange and Innovation Conference on Engineering & Sciences (IEICES). 11, pp.1-7, 2025-10-30. International Exchange and Innovation Conference on Engineering & Sciences
バージョン：

Fenton-like reaction enhanced the CO_2 capture performance of biomass carbon

Xiaoran He[1, 2], Taibao Zhao[2,3], Md. Amirul Islam[2,3], Bidyut Baran Saha[2,3], Osama Eljamal[1]*
[1]Water and Environmental Engineering Laboratory, Interdisciplinary Graduate School of Engineering Sciences, Kyushu University, 6-1 Kasuga-Koen Kasuga, Fukuoka 816-8580, Japan
[2]International Institute for Carbon-Neutral Energy Research (WPI-I2CNER), Kyushu University, 744 Motooka, Nishi-ku, Fukuoka 819-0395, Japan
[3]Department of Mechanical Engineering, Kyushu University, 744 Motooka, Nishi-ku, Fukuoka 819-0395, Japan
*Corresponding author email: osama-eljamal@kyudai.jp

Abstract: *The increasing CO_2 concentration has prompted global efforts to develop efficient CO_2 capture technologies. Biomass carbon is a prospective adsorbent due to its renewability, low cost, and tunable physicochemical properties. However, conventional KOH activation usually requires excessive usage of chemicals, leading to high costs and environmental concerns. In this study, we explore the potential of Fenton-like oxidation to enhance the CO_2 uptake of biomass carbon. The incorporation of transition metal catalysts (Fe, Cu, Mn, Co) into the Fenton-like reaction significantly modifies the carbon structure and introduces oxygen-containing functional groups. The involvement of Mn increased the CO_2 uptake by 47.7% over the original carbon. The results indicate that oxidative pretreatment improves the pore structure and enhances the surface chemistry. The optimal porous carbon reaches a CO_2/N_2 selectivity of 13.75, which is superior to the commercial activated carbon. These insights provide a novel approach for optimizing biomass carbon for sustainable CO_2 capture.*

Keywords: Biomass carbon; CO_2 capture; CO_2/N_2 selectivity; Fenton-like reaction; KOH activation.

1. INTRODUCTION

The alarming increase in atmospheric CO_2 concentration is a major cause of climate change, which urgently requires improved carbon capture and storage (CCS) technologies [1][2]. Among the various strategies, adsorption through porous carbon materials has received much focus due to its energy efficiency, cost-effectiveness, and environmental sustainability [3][4]. Biomass-derived activated carbon (AC) is particularly promising because of its abundant pore structure and properties in terms of surface chemistry [5]. However, optimizing their adsorption performance remains a challenge, especially to minimize production costs while improving CO_2 selectivity.

Conventional activation methods, such as KOH [6]or $ZnCl_2$ [7] activation, can effectively produce high surface areas and porous structures. However, they typically require large amounts of activators, which leads to increased costs and waste disposal issues [8][9]. To address these challenges, oxidative pretreatment approaches, including Fenton and Fenton-like reactions, have been investigated as a means to modify the physicochemical properties of carbon precursors before activation [10][30].

Fenton and Fenton-like reactions involve the catalytic decomposition of H_2O_2 in the presence of transition metals (e.g., Fe, Cu, Mn, and Co) to produce hydroxyl radicals (·OH) [11][12][13]. Due to their favorable one-electron reduction potentials, these ·OH radicals can selectively oxidize functional groups such as C=C, C-H, phenols, aldehydes, ketones, and ether bonds [14][31]. Through introducing oxygen-containing functional groups, the process not only alters the chemical reactivity of the carbon precursor, but also facilitates the subsequent carbonation and activation processes [15][32]. This implies that it is possible to use less KOH to achieve a satisfactory CO_2 capture performance. It makes the process more sustainable and cost-effective and is expected to yield a highly developed, porous activated carbon.

Despite encouraging results from previous investigations, a detailed understanding of the effect of Fenton-like oxidation on biomass carbon is still limited. Therefore, this study aims to systematically investigate the effect of Fenton-like oxidation on the pore structure and CO_2 adsorption capacity of the carbon. The optimized material exhibited excellent CO_2 adsorption capacity, reaching 3.5 mmol g^{-1} at 25 °C and 1 bar, with a CO_2/N_2 selectivity as high as 13.75. Remarkably, the adsorption capacity of the porous carbon remained at 95% after 10 adsorption-desorption cycles. Consequently, the porous carbon synthesized in this study has the potential to serve in large-scale CO_2 capture applications.

2. MATERIALS AND METHODS

2.1 Materials

Pinecones were collected from the local coast of Fukuoka County, Japan, and are required to be washed, dried, and crushed before utilization. HCl (1 mol L^{-1}), KOH, H_2O_2 (30%), copper(II) chloride dehydrate ($CuCl_2{\cdot}2H_2O$, 99.0%), manganese(II) chloride tetrahydrate ($MnCl_2{\cdot}4H_2O$, 99%), cobalt(II) chloride hexahydrate ($CoCl_2{\cdot}6H_2O$, 99%), iron(III) chloride hexahydrate ($FeCl_3{\cdot}6H_2O$, 99%) was purchased from FUJIFILM Wako Pure Chemical Corporation, Japan.

2.2 Preparation process

The biomass was impregnated in a 0.3 mol L^{-1} solution of $CuCl_2{\cdot}2H_2O$, $MnCl_2{\cdot}4H_2O$, $FeCl_3{\cdot}6H_2O$, and $CoCl_2{\cdot}6H_2O$, respectively, and dried after stirring for 24 h. It was then dispersed in 5 wt% H_2O_2 solution, stirred for 24 h, and dried to obtain the carbon precursor. To

prepare the carbon, the above precursors were transferred to a tube furnace and heated at 600 °C in an N_2 atmosphere at 5 °C min^{-1} for 1 h. The obtained product was milled with a planetary ball grinder for 30 min to increase the specific surface area of the carbon and optimize its pore structure. Afterwards, it was activated with KOH in the ratio of 1:1.5 for 2 h at 800 °C (heating rate was 10 °C min^{-1}). Finally, the obtained products were washed repeatedly with deionized water and HCl to remove excess impurities and then dried. The final samples were named metal-AC (metal stands for Cu, Mn, Co, and Fe, respectively). For comparison, a similar procedure was followed for the direct carbonization and activation procedure of the pinecone biomass, but with an activation ratio of 1:3, designated as PC. **Fig. 1.** presents the schematic diagram of the Fenton-like modified carbon synthesis.

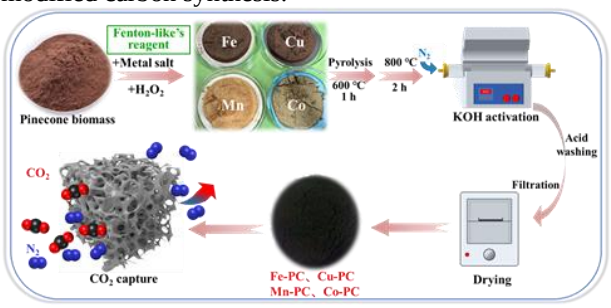

Fig. 1. The synthesis process of the Fenton-like modified carbon.

2.3 Characterization

Scanning Electron Microscopy (SEM, JSM-7900F) was employed to observe the surface morphology and structure of the samples, and Energy Dispersive X-ray Spectroscopy (EDX) was used to confirm the elemental composition and distribution in the samples. The N_2 adsorption-desorption curves were measured with a Belsorp adsorption analyzer, and the pore size distribution was analyzed by the NLDFT method. Here, the microporous volume (V_{micro}) was analyzed using the t-plot model. The ultra-microporous volume ($V_{ultramicro}$) was obtained with the D-R model based on CO_2 adsorption data at 25 °C [16].

2.4 CO_2 adsorption testing

The CO_2 adsorption isotherms were measured using a 3Flex analyzer with all samples' adsorption data from pressure 0 to 110 kPa. The isotherm data were fitted with three adsorption models, respectively.

The Langmuir model is suitable for describing monolayer adsorption on homogeneous surfaces:

$$Q_e = \frac{Q_{max} K_L p}{1 + K_L p} \quad (1)$$

The Freundlich model is commonly used to depict physical adsorption on multilayered or inhomogeneous surfaces:

$$Q_e = K_F p^n \quad (2)$$

The D-R model is mainly applied to microporous filling processes and is suitable for describing low-pressure CO_2 adsorption:

$$Q_e = Q_{max} \exp(-B \ln(\frac{p_0}{p})^2) \quad (3)$$

where K_L (kPa^{-1}) and K_F (kPa^{-1}) are the equilibrium constants of Langmuir and Freundlich models; B (mol^2 kJ^{-2}) is an empirical constant of the D-R model; n refers to temperature-related heterogeneity factor; Q_{max} (mmol g^{-1}) is the maximum adsorption capacity; and Q_e (mmol g^{-1}) refers to the equilibrium adsorption capacity at determined pressure.

Based on the adsorption isotherm data, the Clausius-Clapeyron equation was used to calculate the adsorption heat of the samples with the following equation:

$$Q_{st} = |\Delta H| = RT^2 \left[\frac{\partial \ln p}{\partial T} \right]_n \quad (4)$$

Equation 4 can be morphed into the following form:

$$\ln p = \frac{\Delta H}{RT} + C \quad (5)$$

where T (K) is the absolute temperature during adsorption, p (Pa) is the absolute pressure during adsorption, and R is the gas constant (8.314 J mol^{-1} k^{-1}).

The adsorption selectivity of CO_2/N_2 is significant for the practical application of adsorbents [17]. The Ideal Adsorption Solution Theory (IAST) model is commonly used to predict two-component adsorption results [18].

$$S_{CO_2/N_2} = \frac{q_{CO_2} q_{N_2}}{p_{CO_2} p_{N_2}} \quad (6)$$

where q_{CO2} and q_{N2} are the adsorption capacity of CO_2 and N_2, derived from the single component sorption isotherm, and the CO_2 (0.15 bar) and N_2 (0.85 bar) partial pressures in the flue gas are denoted by p_{CO2} and p_{N2}, respectively.

In addition, the cyclic regeneration of biomass carbon was assessed by 10 adsorption-desorption cycles.

3. RESULTS AND DISCUSSION

3.1 Characterization of the activated carbon

Fig. 2. exhibited the SEM and its corresponding elemental distribution of four metal-modified activated carbon materials (Co-PC, Cu-PC, Fe-PC, and Mn-PC).

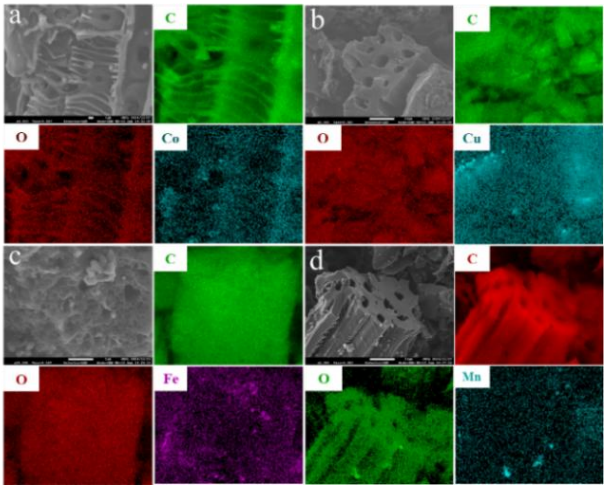

Fig. 2. The SEM and EDX images of (a) Co-PC; (b) Cu-PC; (c) Fe-PC; (d) Mn-PC

The structures of all the samples showed irregular rough surfaces and exhibited a typical porous structure with a more uniform pore distribution. This indicated that Fenton-like reagent pretreatment could strengthen the pore structure of the activated carbon. The EDX results showed that the four metal elements were uniformly distributed on the carbon surface without obvious agglomeration, indicating that the metal loading was relatively homogeneous. In addition, the presence of oxygen elements suggested the existence of oxidized groups on the surface of the material, which contributed to enhancing the adsorption performance or catalytic activity. Overall, the characterization results demonstrated that the metal elements were uniformly distributed on the surface of the activated carbon, and the porous structure of the carbon was maintained.

Fig. 3a showed the N_2 adsorption-desorption isotherms of pristine activated carbon (PC) and four types of Fenton's reagent-modified activated carbons. The PC exhibited higher N_2 adsorption, especially in the low-pressure region ($P/P_0 < 0.1$), with a rapid increase in the adsorption, indicating a well-developed microporous structure. The adsorption capacity of metal-PC was decreased compared to PC, which was directly correlated to the amount of activator KOH. All the carbons were adsorbed in the medium and high-pressure region ($P/P_0 > 0.4$), and the adsorption amounts gradually increased, showing a typical type IV isotherm, which reflected the existence of a composite pore structure of micropores and mesopores in the materials.

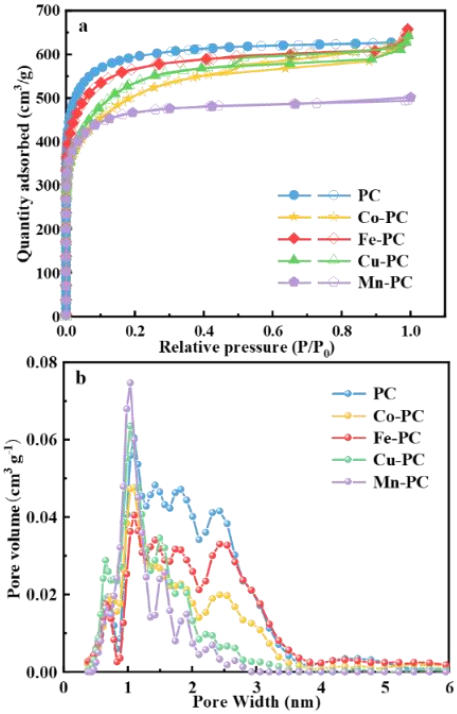

Fig. 3. (a) The N_2 adsorption-desorption isotherms; (b) pore size distributions of different samples.

Fig. 3b displayed the pore size distribution curves for each material. The pore sizes of all the samples were concentrated around 1 nm, and 2~4 nm corresponded to mesopores, mainly dominated by micropores. However, the total pore volume of the Fenton-like reagent-treated samples decreased significantly, indicating that the metal loading blocked some of the micropores to a certain degree, and the pore size distribution was slightly shifted to smaller sizes. Combined with the description of the pore structure parameters in **Table 1**, although the total pore volume and specific surface area decreased, the ultramicroporous volume ($V_{ultramicro<1\ nm}$) of both Mn-PC and Fe-PC was higher than the original PC. This suggested that the Fenton-like pretreatment might have enhanced the partial oxidation on the material surface and formed more ultramicropores. It can be concluded that the Fenton-like pretreatment changed the pore structure of the activated carbon, which is expected to have superior performance in CO_2 adsorption.

Table 1. The pore parameters of different carbons.

Samples	S_{BET} ($m^2\ g^{-1}$)	V_t ($cm^3\ g^{-1}$)	V_{micro} ($cm^3\ g^{-1}$)	$V_{ultramicro<1\ nm}$ ($cm^3\ g^{-1}$)
PC	2479.80	0.95	0.90	0.36
Co-PC	1917.33	0.85	0.80	0.43
Fe-PC	2280.73	0.92	0.88	0.53
Cu-PC	2034.00	0.88	0.85	0.42
Mn-PC	1848.80	0.74	0.72	0.58

3.2 CO_2 capture performance

In adsorption applications, the ideal adsorbent generally has these advantages: high adsorption capacity, low cost, excellent selectivity, low energy consumption for desorption, and high cyclic stability [19]. To evaluate the effect of Fenton-like pretreatment on the CO_2 adsorption capacity of biochar, a 3Flex adsorption analyzer was used to measure the CO_2 adsorption capacity of all samples at 298 K and 1 bar. **Fig. 4.** illustrates that the pretreatment effectively enhanced the CO_2 adsorption performance of the biochar because the ·OH generated by the reaction of the metal salt with H_2O_2 had strong oxidizing properties, which was able to change the pore structure of the activated carbon and increase the ultramicropores' volume, and this was in agreement with the BET results [20].

On the other hand, the introduction of metal oxides (e.g., MnO_x, FeO_x, etc.) and oxygen-containing functional groups (e.g., -OH, -COOH) on the biochar surface can increase the alkaline sites, which is favorable for CO_2 adsorption [21]. Among them, the Mn-modified samples showed the best performance, which was consistent with the enhancement of oxidation state and alkaline adsorption sites. Moreover, Mn-PC had the largest ultramicroporous volume. Research has demonstrated that ultramicropores (<1 nm) are the main driving force for CO_2 adsorption, whereas pores larger than three times the CO_2 molecule diameter (~0.33 nm) contribute little to adsorption [22]. Consequently, the volume of the ultramicropores and the alkaline sites are the main factors affecting the CO_2 adsorption performance.

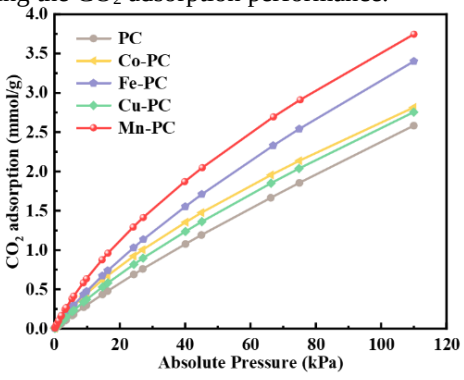

Fig. 4. The CO_2 adsorption isotherms of all samples.

Fig. 5. exhibited the adsorption isotherms of the four modified activated carbons at different temperatures. As the temperature increased from 278.15 K to 298.15 K, the CO_2 adsorption of all four samples decreased, which indicated that the adsorption was an exothermic process.

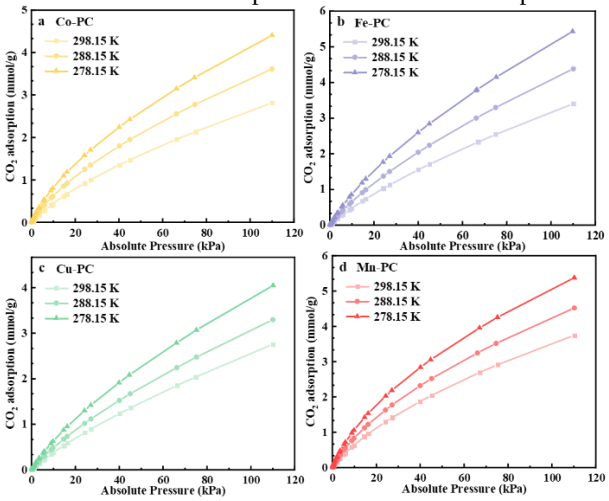

Fig. 5. The CO_2 adsorption isotherms under different temperatures.

Fig. 6. presented the CO_2 adsorption on Mn-PC fitted by three isothermal adsorption models. The parameters obtained from the fitting are summarized in **Table 2**. In general, lower chi-square (χ^2) values represent higher fitting accuracy [23][24]. As can be seen from **Table 2**, the χ^2 values of the Freundlich model were lower than the Langmuir model, which indicated that physical adsorption might play a dominant role in CO_2 adsorption. In addition, the D-R model showed the lowest $\chi 2$ value and the closest R^2 to 1, suggesting that both physical and chemical adsorption occurred. It was notable that the presence of metallic elements could effectively enhance the chemisorption of CO_2 on porous carbon by increasing the alkaline active sites [25].

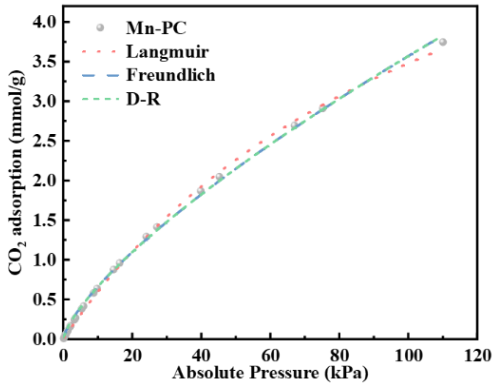

Fig. 6. Fitting curves of three adsorption models.

Table 2. Model fitting parameters of CO_2 adsorption isotherms on Mn-PC.

Models	Fitted Parameters	Temperature (298.15 K)
Langmuir	Q_{max} (mmol g^{-1})	7.553
	K_L (kPa^{-1})	0.00854
	R^2	0.9985
	χ^2	0.0017
Freundlich	K_F (mmol g^{-1} kPa^{-n})	0.12219
	n	0.733
	R^2	0.9987
	χ^2	0.0015
Dubinin-Radushkevich (D-R)	Q_{max} (mmol g^{-1})	7.5934
	B (mol^2 kJ^{-2})	0.366
	R^2	0.9990
	χ^2	0.0013

The adsorption heat (Q_{st}) was calculated according to Eqs. (4) - (5) based on the CO_2 adsorption data at different temperatures. **Fig. 7 (a)** presented the relationship between ln P and 1/T, with different color curves corresponding to different adsorption amounts (mmol g^{-1}). All curves presented negative slopes, which indicated that the CO_2 adsorption on Mn-PC was an exothermic process.

According to the Clausius-Clapeyron equation, the slope of the fitted line can be used to calculate Q_{st}. Q_{st} was higher at low adsorption amounts, implying that there was a stronger interaction between carbon and CO_2 molecules at the initial stage, which may be related to the enhanced surface polarity due to Mn modification [26][27]. However, Q_{st} decreased with increasing adsorption amount, implying that the strong, active sites were gradually occupied and the adsorption was saturated [28]. The Q_{st} of Mn-PC ranged from about 18 to 28 kJ mol^{-1}, which indicated that its CO_2 adsorption was mainly physisorption. This revealed that the Mn-PC had a good regenerative property and was able to maintain a low energy consumption in the adsorption-desorption cycle. Consequently, this material has an excellent potential for industrial applications.

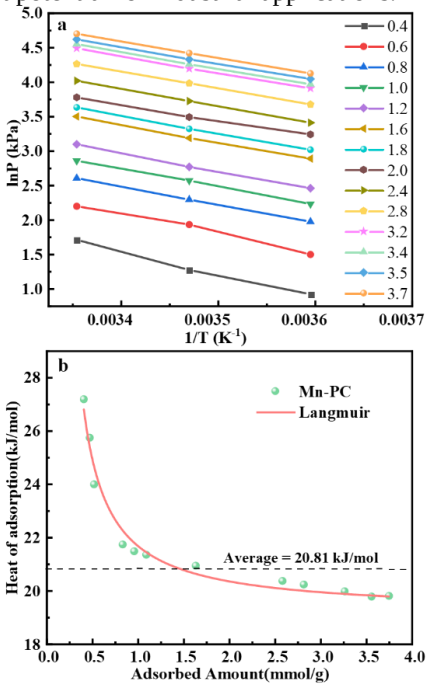

Fig. 7. (a) Relationship between ln P and 1/T of Mn-PC at different adsorption amount; (b) Heat of CO_2 adsorption of Mn-PC.

To assess the CO_2/N_2 separation performance of the modified activated carbon, the N_2 adsorption isotherms of all samples were tested at 298 K and 1 bar. Obviously, the N_2 adsorption capacity of each sample was much lower than the CO_2 adsorption capacity at the same temperature and pressure. The selectivity was calculated according to the IAST model, which can effectively predict the adsorption selectivity of the adsorbent for any

binary gas mixture, where the mixture composition simulated the post-combustion flue gas composition (CO_2/N_2=15/85) [29].

Fig. 8b showed that the Mn-modified material exhibited the highest selectivity of 13.75 for CO_2, which was probably related to the modulation of the surface charge distribution of the material by Mn, enhancing the interaction between CO_2 and the adsorption sites. In addition, the Mn and Co modifications significantly increased the selectivity of the materials for CO_2, which was attributed to the fact that the modification of the metal atoms may produce more polar sites or defects on the surface of the materials, increasing the adsorption capacity of CO_2 molecules, while decreasing the competing adsorption of N_2. The results suggest that Mn-PC is suitable for simulated flue gas separation or low concentration CO_2 capture applications.

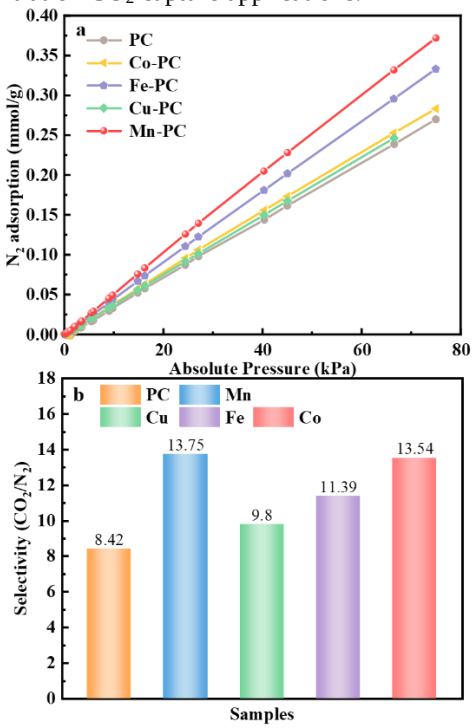

Fig. 8. (a) The N_2 adsorption isotherms of different samples; (b) CO_2/N_2 adsorption selectivity of metal-PC.

The CO_2 desorption curve of Mn-PC at 298 K was examined in **Fig. 9**. In comparison with the adsorption curve, it can be seen that the adsorption-desorption process was shown to be almost reversible. It proved that the vacuum desorption process could effectively remove nearly all the CO_2 on the surface and inside the pores of Mn-PC.

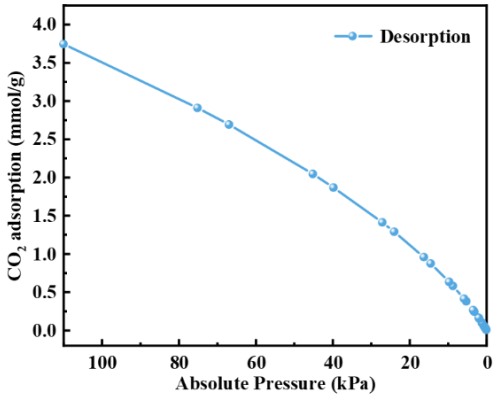

Fig. 9. The CO_2 desorption curves of Mn-PC.

The ideal adsorbent requires not only high adsorption capacity and selectivity but also recoverability, which is the key to determining its practical application value. After the adsorption reached equilibrium, the adsorbent was placed under vacuum and degassed for 2 h for the next adsorption. **Fig. 10.** demonstrated the experimental data of CO_2 adsorption for 10 adsorption-desorption cycles, and the CO_2 adsorption capacity did not decrease significantly, indicating its excellent recoverability.

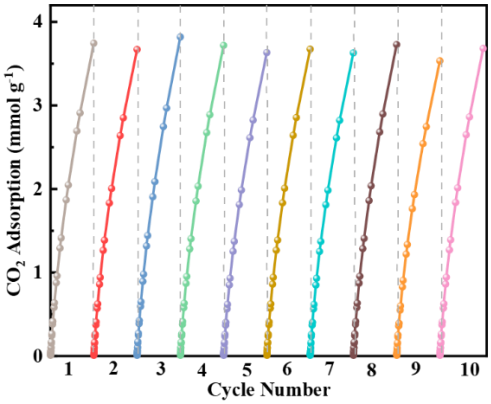

Fig. 10. The cycle performance of Mn-PC at 1 bar and 298.15 K.

4. CONCLUSIONS

In this study, a series of metal-assisted Fenton-like pretreatment strategies were developed to enhance the CO_2 adsorption performance of biomass-derived activated carbon. The introduction of transition metal catalysts (Fe, Cu, Mn, Co) not only tailored the pore structure but also enriched the surface chemistry with oxygen-containing and alkaline functional groups, which significantly contributed to the adsorption efficiency.

Among all samples, Mn-modified activated carbon (Mn-PC) exhibited the most promising performance. It achieved a CO_2 uptake of 3.5 mmol g^{-1} at 25 °C and 1 bar, representing a 47.7% increase compared to the pristine sample (PC). Additionally, the CO_2/N_2 selectivity reached 13.75, outperforming commercial activated carbon. The enhanced performance is mainly attributed to the increased ultramicropore volume (0.58 cm^3 g^{-1} for Mn-PC vs. 0.36 cm^3 g^{-1} for PC) and the introduction of alkaline sites by Mn species. Furthermore, Mn-PC demonstrated excellent cyclic stability, maintaining 95% of its initial adsorption capacity after 10 consecutive cycles, and exhibited reversible adsorption-desorption behavior under vacuum conditions.

Overall, this work confirms that Fenton-like pretreatment, particularly with Mn catalysts, is a viable and green strategy to enhance the CO_2 capture capacity and selectivity of biomass-based porous carbons. The results offer a scalable pathway for designing low-cost, high-performance adsorbents for post-combustion CO_2 separation.

5. REFERENCES

[1] Wanlin, G., Shuyu, L., Rujie, W., Qian, J., Yu, Z., Qianwen, Z., Bingqiao, X., Cui Ying, T., and Zhu, X., 2020, "Industrial Carbon Dioxide Capture and Utilization: State of the Art and Future Challenges," Chem. Soc. Rev., **49**(23), pp. 8584–8686.

[2] Mohd Faizul, I., Falyouna, O., and Eljamal, O., 2021, "Effect of Graphene Oxide Synthesis Method on the Adsorption Performance of Pharmaceutical Contaminants," Proc. Int. Exch. Innov. Conf. Eng. Sci., **7**, pp. 232–239.

[3] Xiaoran, H., Eljamal, O., and Bidyut Baran, S., 2024, "Modified Biochar for Antibiotics Removal in Aqueous Environments: A Mini Review," Proc. Int. Exch. Innov. Conf. Eng. Sci., **10**, pp. 156–163.

[4] Khalil, A. M. E., Han, L., Maamoun, I., Tabish, T. A., Chen, Y., Eljamal, O., Zhang, S., Butler, D., and Memon, F. A., 2022, "Novel Graphene-Based Foam Composite as a Highly Reactive Filter Medium for the Efficient Removal of Gemfibrozil from (Waste)Water," Adv. Sustain. Syst., **6**(8), p. 2200016.

[5] Md. Amirul, I., and Bidyut Baran, S., 2024, "Optimal Utilization of Waste Biomass for the Development of Minimal Emission Sustainable Cooling Systems," *Advancements in Non-Conventional Cooling and Thermal Storage Strategies*, Wiley, pp. 39–63.

[6] He, X., Islam, M. A., Zhao, T., Eljamal, O., and Saha, B. B., 2025, "KOH-activated Pinecone Biochar for Efficient Chloramphenicol Removal from Aqueous Solutions," CleanMat.

[7] Guo, T., Tian, W., and Wang, Y., 2022, "Effect of Pore Structure on CO2 Adsorption Performance for ZnCl2/FeCl3/H2O(g) Co-Activated Walnut Shell-Based Biochar," Atmosphere (Basel)., **13**(7), p. 1110.

[8] Islam, M. A., Yoon, S.-H., Miyawaki, J., and Saha, B. B., 2024, "Activated Carbon Derived from Waste Mangrove Biomass for Designing Heat Pumps with Improved Specific Cooling Capacity and Lower CO2 Emission," Int. Commun. Heat Mass Transf., **158**, p. 107828.

[9] Assilbekov, B., Pal, A., Islam, M. A., and Saha, B. B., 2024, "Investigation of Mass Transport Characteristics of CO2 Adsorption onto Activated Carbon: An Experimental and Numerical Study," Int. Commun. Heat Mass Transf., **157**, p. 107779.

[10] Li, Y., Ni, L., Luo, J., Zhu, L., Zhang, X., Li, H., Zada, I., Yu, J., Zhu, S., Lian, K., Li, Y., and Zhang, D., 2024, "Fenton Reaction Doubled Biomass Carbon Activation Efficiency for High-Performance Supercapacitors," Adv. Funct. Mater., **34**(39), p. 2403448.

[11] Zhang, M., Dong, H., Zhao, L., Wang, D., and Meng, D., 2019, "A Review on Fenton Process for Organic Wastewater Treatment Based on Optimization Perspective," Sci. Total Environ., **670**, pp. 110–121.

[12] Kazimierowicz, J., Dębowski, M., and Zieliński, M., 2023, "Effect of Pharmaceutical Sludge Pre-Treatment with Fenton/Fenton-like Reagents on Toxicity and Anaerobic Digestion Efficiency," Int. J. Environ. Res. Public Health, **20**(1).

[13] Wang, J., and Wang, S., 2020, "Reactive Species in Advanced Oxidation Processes: Formation, Identification and Reaction Mechanism," Chem. Eng. J., **401**, p. 126158.

[14] Di Tommaso, S., Rotureau, P., Crescenzi, O., and Adamo, C., 2011, "Oxidation Mechanism of Diethyl Ether: A Complex Process for a Simple Molecule," Phys. Chem. Chem. Phys., **13**(32), p. 14636.

[15] Zhou, H., Zhang, H., He, Y., Huang, B., Zhou, C., Yao, G., and Lai, B., 2021, "Critical Review of Reductant-Enhanced Peroxide Activation Processes: Trade-off between Accelerated Fe3+/Fe2+ Cycle and Quenching Reactions," Appl. Catal. B Environ., **286**, p. 119900.

[16] Zhou, J., Li, Z., Xing, W., Shen, H., Bi, X., Zhu, T., Qiu, Z., and Zhuo, S., 2016, "A New Approach to Tuning Carbon Ultramicropore Size at Sub-Angstrom Level for Maximizing Specific Capacitance and CO2 Uptake," Adv. Funct. Mater., **26**(44), pp. 7955–7964.

[17] Yang, P., Rao, L., Zhu, W., Wang, L., Ma, R., Chen, F., Lin, G., and Hu, X., 2020, "Porous Carbons Derived from Sustainable Biomass via a Facile One-Step Synthesis Strategy as Efficient CO2 Adsorbents," Ind. Eng. Chem. Res., **59**(13), pp. 6194–6201.

[18] Khosrowshahi, M. S., Mashhadimoslem, H., Shayesteh, H., Singh, G., Khakpour, E., Guan, X., Rahimi, M., Maleki, F., Kumar, P., and Vinu, A., 2023, "Natural Products Derived Porous Carbons for CO2 Capture," Adv. Sci., **10**(36), p. 2304289.

[19] Dziejarski, B., Serafin, J., Andersson, K., and Krzyżyńska, R., 2023, "CO2 Capture Materials: A Review of Current Trends and Future Challenges," Mater. Today Sustain., **24**, p. 100483.

[20] Tang, J., and Wang, J., 2018, "Fenton-like Degradation of Sulfamethoxazole Using Fe-Based Magnetic Nanoparticles Embedded into Mesoporous Carbon Hybrid as an Efficient Catalyst," Chem. Eng. J., **351**, pp. 1085–1094.

[21] Zhao, Y., and Liu, Y., 2022, "Preparation of Hydrogen Sulfide Adsorbent Derived from Spent Fenton-like Reagent Modified Biochar and Its Removal Characteristics for Hydrogen Sulfide," Fuel Process. Technol., **238**, p. 107495.

[22] Durán-Jiménez, G., Stevens, L. A., Kostas, E. T., Hernández-Montoya, V., Robinson, J. P., and Binner, E. R., 2020, "Rapid, Simple and Sustainable Synthesis of Ultra-Microporous Carbons with High Performance for CO2 Uptake, via Microwave Heating," Chem. Eng. J., **388**, p. 124309.

[23] Xiao, J., Yuan, X., Zhang, T. C., Ouyang, L., and Yuan, S., 2022, "Nitrogen-Doped Porous Carbon for Excellent CO2 Capture: A Novel Method for Preparation and Performance Evaluation," Sep. Purif. Technol., **298**, p. 121602.

[24] Wu, C., Zhang, G., Liu, J., Wang, Y., Zhao, Y., and Li, G., 2023, "A Green Strategy to Prepare Nitrogen-Oxygen Co-Doped Porous Carbons from Macadamia Nut Shells for Post-

Combustion CO2 Capture and Supercapacitors," J. Anal. Appl. Pyrolysis, **171**, p. 105952.

[25] He, G., Yuan, X., Wang, Y., Yilmaz, M., Li, J., and Yuan, S., 2025, "N, S-Codoped Porous Biochar Derived from Bagasse-Based Polycondensate for High-Performance CO2 Capture and Supercapacitor," Sep. Purif. Technol., **354**, p. 128826.

[26] Cao, M., Shu, Y., Bai, Q., Li, C., Chen, B., Shen, Y., and Uyama, H., 2023, "Design of Biomass-Based N, S Co-Doped Porous Carbon via a Straightforward Post-Treatment Strategy for Enhanced CO2 Capture Performance," Sci. Total Environ., **884**, p. 163750.

[27] Bai, J., Shao, J., Yu, Q., Demir, M., Nazli Altay, B., Muhammad Ali, T., Jiang, Y., Wang, L., and Hu, X., 2024, "Sulfur-Doped Porous Carbon Adsorbent: A Promising Solution for Effective and Selective CO2 Capture," Chem. Eng. J., **479**, p. 147667.

[28] Shao, J., Wang, J., Yu, Q., Yang, F., Demir, M., Altinci, O. C., Umay, A., Wang, L., and Hu, X., 2024, "Unlocking the Potential of N-Doped Porous Carbon: Facile Synthesis and Superior CO2 Adsorption Performance," Sep. Purif. Technol., **333**, p. 125891.

[29] Shi, W., Wang, R., Liu, H., Chang, B., Yang, B., and Zhang, Z., 2019, "Biowaste-Derived 3D Honeycomb-like N and S Dual-Doped Hierarchically Porous Carbons for High-Efficient CO2 Capture," RSC Adv., **9**(40), pp. 23241–23253.

[30] O. Eljamal, K. Sasaki, T. Hirajima, Sorption kinetic of arsenate as water contaminant on zero valent iron, J. Water Resour. Prot. 5 (2013) 563–567.

[31] O. Eljamal, J. Okawauchi, K. Hiramatsu, Removal of phosphorus from water using marble dust as sorbent material, J. Environ. Prot. 3 (2012) 709–714.

[32] B. Singha, S.C. Karmaker, O. Eljamal, Quantifying the direct and indirect effect of socio-psychological and behavioral factors on residential water conservation behavior and consumption in Japan, Resour. Conserv. Recycl. 190 (2023) 106816.